

PACS numbers: 42.55.Rz; 42.60.Da; 42.60.Mi
DOI: 10.1070/QE2008v038n11ABEH013844

Vector model of a ring solid-state laser taking into account the spatial inhomogeneity of the pump and radiation field

D.A. Aleshin, N.V. Kravtsov, E.G. Lariontsev, S.N. Chekina

***Abstract*. A system of equations of the vector model of ring solid-state lasers is derived taking into account the inhomogeneity of the pump transverse distribution and fields of counterpropagating waves. The model under study well describes the experimental dependence of the phase shift of self-modulations oscillations on the pump excess over the threshold. It is shown that the inhomogeneity of the transverse distributions of fields of counterpropagating waves and the inhomogeneity of the permittivity of the intracavity medium can lead to the appearance of frequency and amplitude nonreciprocities in a solid-state laser.**

Keywords: *solid-state ring laser, vector model, self-modulation oscillations, nonreciprocal effects.*

1. Introduction

A solid-state ring laser (SRL) is a complex nonlinear system in which many different lasing regimes, both regular and chaotic, can appear. All the main features of the nonlinear dynamics of this laser can be qualitatively described by using a rather simple so-called standard theoretical model (see reviews [1, 2]). Its basic equations are derived under the assumptions which are usually not fulfilled in real lasers but considerably simplify the mathematical model:

(i) the wave polarisation is assumed linear and the same for counterpropagating waves;

(ii) the plane-wave approximation is used for the intracavity field;

(iii) the spatial inhomogeneity of the population inversion and the pump in the direction perpendicular to the resonator axis is neglected.

To achieve the quantitative agreement with the experiment, some simplifying assumptions should be discarded. Thus, vector models taking into account the difference between elliptic polarisations of counterpropagating waves were proposed and used in papers [3 – 6]. Although these vector models gave a better quantitative agreement between the theory and the experiment, the problem of the development of the mathematical model adequately describing the SRL dynamics has not been solved so far.

Such a mathematical model is necessary, for example, to formulate and solve inverse problems. In science and technology, the solution of inverse problems is required to calculate the system parameters, which cannot be measured directly. In laser physics, the use of inverse problems allows one to determine laser parameters by the peculiarities of their dynamic behaviour.

The aim of this paper is to improve the vector model proposed in [4] by taking into account the spatial inhomogeneity of the pump intensity and the intracavity laser radiation field.

D.A. Aleshin, N.V. Kravtsov, E.G. Lariontsev, S.N. Chekina
D.V. Skobeltsyn Institute of Nuclear Physics, M.V. Lomonosov Moscow State University, Vorobevy gory, 119992 Moscow, Russia;
e-mail: e.lariontsev@yahoo.com, kravtsov@npi.phys.msu.su

Received 20 March 2008; revision received 22 May 2008
Kvantovaya Elektronika **38** (11) 1016 – 1020 (2008)
Translated by I.A. Ulitkin

2. Derivation of basic equations of the vector model

As a rule, to describe the SRL dynamics, a semiclassical theory is used, which is based on Maxwell's equations for the intracavity field and on the system of quantum-mechanical equations for the density matrix of active atoms.

Maxwell's equations for the intracavity field in the cgs system have the form:

$$\varepsilon\frac{\partial^2\boldsymbol{E}(\boldsymbol{r},t)}{\partial t^2}+4\pi\sigma\frac{\partial\boldsymbol{E}(\boldsymbol{r},t)}{\partial t}-c^2\Delta\boldsymbol{E}(\boldsymbol{r},t)$$

$$-2([\dot{\boldsymbol{\theta}}\boldsymbol{r}]\mathrm{grad})\frac{\partial\boldsymbol{E}(\boldsymbol{r},t)}{\partial t}=-4\pi\frac{\partial^2\boldsymbol{P}_{\mathrm{a}}(\boldsymbol{r},t)}{\partial t^2}, \qquad (1)$$

where $\boldsymbol{E}(\boldsymbol{r},t)$ is the vector of the intracavity electric field strength; ε is the medium permittivity; σ is the medium conductivity; c is the speed of light in vacuum; $\dot{\boldsymbol{\theta}}$ is the angular velocity of the cavity rotation; and $\boldsymbol{P}_{\mathrm{a}}$ is the vector of the medium polarisation.

The equations for the nondiagonal elements ρ_{ab} and ρ_{ba} of the density matrix of active atoms and for the population inversion in a two-level medium can be written in the form

$$\left(\frac{\partial}{\partial t}+\mathrm{i}\omega_0+\gamma_{\mathrm{ab}}\right)\rho_{\mathrm{ab}}=\frac{\mathrm{i}}{\hbar}\,\boldsymbol{d}_{\mathrm{ab}}(\rho_{\mathrm{b}}-\rho_a)\boldsymbol{E}, \qquad (2)$$

$$\frac{\partial N}{\partial t}=W-\frac{N}{T_1}+\mathrm{i}\,\frac{n_0}{\hbar}(\boldsymbol{d}_{\mathrm{ab}}\rho_{\mathrm{ba}}-\rho_{\mathrm{ab}}\boldsymbol{d}_{\mathrm{ba}})\boldsymbol{E}, \qquad (3)$$

where ω_0 is the frequency of the quantum transition from the level a to the level b; T_1 is the longitudinal relaxation time; γ_{ab} is the relaxation rate of the medium polarisation; $\hbar$

is Planck's constant; $\boldsymbol{d}_{ab}$ is the matrix element of the atomic dipole moment operator; $N = n_0(\rho_b - \rho_a)$ is the population inversion of working levels; ρ_a and ρ_b are diagonal elements of the density matrix; n_0 is the density of the number of active atoms; and W is the pump rate.

The permittivity of the intracavity medium can be written in the form

$$\varepsilon(\boldsymbol{r}) = \varepsilon_c + \delta\varepsilon(\boldsymbol{r}),$$

where ε_c characterises the homogeneous medium completely filling the resonator (we consider a monolithic laser) and the addition $\delta\varepsilon(\boldsymbol{r})$ describes the inhomogeneities, which can cause the backscattering of radiation and coupling of counterpropagating waves. In addition, $\delta\varepsilon(\boldsymbol{r})$ includes the change in the permittivity due to the population caused by pumping the nonresonance levels of active centres.

The quantity $\delta\varepsilon(\boldsymbol{r})$ is assumed small and considered as a perturbation. The intracavity losses and radiation amplification per round-trip in the cavity are also assumed small. By transferring all the small terms in expression (1) to the right-hand side and dividing this equation by ε_c, we obtain

$$\frac{\partial^2 \boldsymbol{E}(\boldsymbol{r},t)}{\partial t^2} - \frac{c^2}{\varepsilon_c}\Delta\boldsymbol{E}(\boldsymbol{r},t) = -\frac{4\pi}{\varepsilon_c}\frac{\partial^2 \boldsymbol{P}_a(\boldsymbol{r},t)}{\partial t^2} - \frac{\delta\varepsilon}{\varepsilon_c}\frac{\partial^2 \boldsymbol{E}(\boldsymbol{r},t)}{\partial t^2}$$

$$-4\pi\frac{\sigma(\boldsymbol{r})}{\varepsilon_c}\frac{\partial \boldsymbol{E}(\boldsymbol{r},t)}{\partial t} + \frac{2}{\varepsilon_c}([\dot{\boldsymbol{\theta}}\boldsymbol{r}]\mathrm{grad})\frac{\partial \boldsymbol{E}(\boldsymbol{r},t)}{\partial t}. \quad (4)$$

By neglecting small terms (the right-hand side), we obtain the equation

$$\frac{\partial^2 \boldsymbol{E}(\boldsymbol{r},t)}{\partial t^2} - \frac{c^2}{\varepsilon_c}\Delta\boldsymbol{E}(\boldsymbol{r},t) = 0, \quad (5)$$

determining the field distribution in the ideal ring cavity without losses and without coupling between counterpropagating waves. In a ring cavity with a nonplanar beam contour, Gaussian beams with a complex astigmatism are produced during the propagation of light inside the cavity and reflections from spherical and plane surfaces (mirrors) [7, 8]. The spatial field distributions of counterpropagating waves in this case are described by the functions

$$u_{1,2}(x,y,z) = A_{1,2}(z)\varphi_{1,2}(x,y,z), \quad (6)$$

where $A_{1,2}(z)$ are complex wave amplitudes;

$$\varphi_{1,2}(x,y,z) = \exp\left[\pm \mathrm{i}k\,\frac{q^x_{1,2}(z)x^2 + 2q^{xy}_{1,2}(z)xy + q^y_{1,2}(z)y^2}{2}\right]; \quad (7)$$

z is the coordinate along the beam propagation; x, y are the transverse coordinates; k is the wave number;

$$\frac{1}{q^j_{1,2}} = \frac{1}{R^j_{1,2}(z)} \pm \frac{2\mathrm{i}}{k[w^j_{1,2}(z)]^2} \quad (j = x, xy, y)$$

are complex parameters of the Gaussian beam; $R^x_{1,2}(z)$, $R^y_{1,2}(z)$ are the radii of the wave front curvature; and $w^x_{1,2}(z)$, $w^y_{1,2}(z)$ are the beam radii along the x and y axes. The parameters $R^{xy}_{1,2}(z)$ and $w^{xy}_{1,2}(z)$ describe the specific nature of the Gaussian beam with a complex astigmatism.

The functions $u_{1,2}(x,y,z)$ are the solutions of the Helmholtz equation

$$\Delta u_{1,2}(x,y,z) + k^2 u_{1,2}(x,y,z) = 0. \quad (8)$$

The eigenvalues of wave numbers k_n and the resonator eigenfrequencies $\omega_n = ck_n/\varepsilon_c^{1/2}$ can be found by using the conditions for the field periodicity in a ring cavity

$$u_{1,2}(x,y,z) = u_{1,2}(x,y,z+L) \quad (9)$$

(L is the perimeter of the beam contour), the conditions for the arbitrary electric (magnetic) field periodicity and the conditions for the reflection at resonator mirrors. The subscript n in k_n and ω_n is omitted below.

By using the Jones matrix method, we can find the polarisation vectors of counterpropagating waves $\boldsymbol{e}_{1,2}(z)$.

We expand the solution of Eqn (4) in the eigenfunctions $u_{1,2}(x,y,z)$ of the ring cavity:

$$\boldsymbol{E}(\boldsymbol{r},t) = \frac{1}{2}\left\{\sum_{1,2} E_{1,2}(t)\boldsymbol{e}_{1,2}(z)u_{1,2}(\boldsymbol{r}) \times \exp[\mathrm{i}(\omega t \pm kz)] + \mathrm{c.c.}\right\}. \quad (10)$$

In the case of solid-state lasers, the medium polarisation is rapidly established and it can be adiabatically excluded. The solution of Eqn (2) in the quasi-static approximations has the form:

$$\rho_{ab} = -\frac{\mathrm{i}}{2n_0\hbar\gamma_{ab}}\frac{N}{1-\mathrm{i}\delta}\boldsymbol{d}_{ab}\sum_{1,2}E_{1,2}(t)\boldsymbol{e}_{1,2}(z)u_{1,2}(\boldsymbol{r}) \times \exp[\mathrm{i}(\omega t \pm kz)], \quad (11)$$

where $\delta = (\omega - \omega_0)/\gamma_{ab}$ is the relative laser frequency detuning ω from the gain line centre. The vector of the medium polarisation is expressed via nondiagonal elements of the density matrix of active atoms:

$$\boldsymbol{P}_a = n_0(\boldsymbol{d}_{ab}\rho_{ba} + \boldsymbol{d}_{ba}\rho_{ab}). \quad (12)$$

By assuming that the active medium is isotropic, we obtain from (11), (12) the expression

$$\boldsymbol{P}_a = -\frac{\mathrm{i}}{2}\frac{|\boldsymbol{d}_{ab}|^2}{\hbar\gamma_{ab}}\frac{N(\boldsymbol{r})}{1+\delta^2}\left\{(1-\mathrm{i}\delta)\sum_{1,2}E_{1,2}(t)\boldsymbol{e}_{1,2}(z)u_{1,2}(\boldsymbol{r}) \times \exp[\mathrm{i}(\omega t \pm kz)] - \mathrm{c.c.}\right\} \quad (13)$$

for the polarisation vector:

By substituting (10) and (13) into (4) in the slowly varying-amplitude approximation $(\mathrm{d}E_{1,2}/\mathrm{d}t \ll \omega E_{1,2})$, we obtain

$$\frac{\mathrm{d}E_{1,2}}{\mathrm{d}t}\boldsymbol{e}_{1,2}(z)u_{1,2}(\boldsymbol{r}) = -\frac{1}{2\varepsilon_c}[\mathrm{i}\omega\delta\varepsilon(\boldsymbol{r}) + 4\pi\sigma(\boldsymbol{r})] \times E_{1,2}\boldsymbol{e}_{1,2}(z)u_{1,2}(\boldsymbol{r}) \pm \frac{\mathrm{i}k}{\varepsilon_c}[\dot{\boldsymbol{\theta}}\boldsymbol{r}]_z E_{1,2}\boldsymbol{e}_{1,2}(z)u_{1,2}(\boldsymbol{r})$$

$$-\frac{1}{2\varepsilon_c}[\mathrm{i}\omega\delta\varepsilon(\boldsymbol{r}) + 4\pi\sigma(\boldsymbol{r})]\exp(\mp 2\mathrm{i}kz)E_{2,1}\boldsymbol{e}_{2,1}(z)u_{2,1}(\boldsymbol{r}) +$$

$$+\frac{2\pi\omega}{\varepsilon_c\hbar\gamma_{ab}}|\boldsymbol{d}_{ab}|^2(1-i\delta)\frac{N}{1+\delta^2}$$

$$\times E_{1,2}\boldsymbol{e}_{1,2}(z)u_{1,2}(\boldsymbol{r})+E_{2,1}\boldsymbol{e}_{2,1}(z)u_{2,1}(\boldsymbol{r})\exp(\mp 2ikz)]. \quad (14)$$

By multiplying (14) by $\boldsymbol{e}^*_{1,2}(z)u^*_{1,2}(\boldsymbol{r})$, we integrate over the resonator volume and use the normalisation

$$\int|u_{1,2}(\boldsymbol{r})|^2d\boldsymbol{r}=1, \quad |\boldsymbol{e}_{1,2}|^2=1 \quad (15)$$

for the polarisation vectors $\boldsymbol{e}_{1,2}(z)$ and eigenfunctions $u_{1,2}(\boldsymbol{r})$. After integrating over the volume, we obtain from (14)

$$\frac{dE_{1,2}}{dt}=-\frac{\omega}{2Q_{1,2}}E_{1,2}-i\left(\omega_{\varepsilon 1,\varepsilon 2}\mp\frac{1}{2}\Omega_{1,2}\right)E_{1,2}$$

$$+\frac{i}{2}\tilde{m}_{1,2}E_{2,1}+\frac{\sigma L}{2T}(1-i\delta)(N_{1,2}E_{1,2}+N_{12,21}E_{2,1}). \quad (16)$$

Here, we introduce the time-dependent variables:

$$N_{1,2}=\int N(\boldsymbol{r})|u_{1,2}(\boldsymbol{r})|^2d\boldsymbol{r}, \quad (17)$$

$$N_{12}=\int N(\boldsymbol{r})u^*_2(\boldsymbol{r})u_1(\boldsymbol{r})[e_1(z)e^*_2(z)],$$

$$\times\exp(2ikz)d\boldsymbol{r}, \quad N_{21}=N^*_{12}. \quad (18)$$

In the particular case, when the resonator eigenfunctions are plane waves, these variables are spatial harmonics of the inverse population [1–4]. In addition, expression (16) involves the following parameters:

$$\sigma=\frac{\sigma_0}{1+\delta^2}=\frac{1}{1+\delta^2}\frac{4\pi\omega|\boldsymbol{d}_{ab}|^2}{\varepsilon_c^{1/2}\hbar\gamma_{ab}} \quad (19)$$

is the laser transition cross section; σ_0 is the cross section at the gain line centre;

$$\frac{\omega}{Q_{1,2}}=\frac{4\pi}{\varepsilon_c}\int\sigma(\boldsymbol{r})|u_{1,2}(\boldsymbol{r})|^2d\boldsymbol{r} \quad (20)$$

are the bandwidths (Q factors $Q_{1,2}$) of the ring cavity for counterpropagating waves;

$$\omega_{\varepsilon 1,\varepsilon 2}=\frac{\omega}{\varepsilon_c}\int\delta\varepsilon(\boldsymbol{r})|u_{1,2}(x,y)|^2d\boldsymbol{r} \quad (21)$$

are the shifts of the ring-cavity eigenfrequencies due to the inhomogeneity of the medium permittivity;

$$\Omega_{1,2}=\pm\frac{2k}{\varepsilon_c}\int[\dot{\boldsymbol{\theta}}\boldsymbol{r}]_z|u_{1,2}(\boldsymbol{r})|^2d\boldsymbol{r} \quad (22)$$

are the shifts of ring-cavity eigenfrequencies for counterpropagating waves due to the resonator rotation; and

$$\tilde{m}_{1,2}=m_{1,2}\exp(\pm i\theta_{1,2})=\frac{1}{\varepsilon_c}\int(\boldsymbol{e}_{2,1}\boldsymbol{e}_{1,2})$$

$$\times[4\pi i\sigma(\boldsymbol{r})-\omega\delta\varepsilon(\boldsymbol{r})]u_{2,1}(\boldsymbol{r})u^*_{1,2}(\boldsymbol{r})\exp(\mp 2ikz)d\boldsymbol{r} \quad (23)$$

are the complex coupling coefficients of counterpropagating waves.

Taking into account (10) and (11), Eqn (3) for the inverse population density assumes the form

$$\frac{\partial N(\boldsymbol{r})}{\partial t}=W-\frac{N(\boldsymbol{r})}{T_1}-\frac{aN(\boldsymbol{r})}{T_1}\left[\sum_{1,2}|E_{1,2}|^2|u_{1,2}(\boldsymbol{r})|^2\right.$$

$$\left.+\sum_{1,2}E_{1,2}E^*_{2,1}(\boldsymbol{e}_{1,2}\boldsymbol{e}_{2,1})u_{1,2}(\boldsymbol{r})u^*_{2,1}(\boldsymbol{r})\exp(\pm 2ikz)\right], \quad (24)$$

where

$$a=\frac{T_1}{1+\delta^2}\frac{|\boldsymbol{d}_{ab}|^2}{2\hbar^2\gamma_{ab}}$$

is the saturation parameter.

Equations (16), (24) represent the system of integro-differential equations. To simulate the SRL emission dynamics in the most general case, it is necessary to solve this particular system of equations. However, in practice it is not always expedient, and good agreement with the experiment can be obtained by making a number of simplifying assumptions and by transforming this system into a system of ordinary differential equations (as is usually done in the standard model).

Let the pump rate be

$$W(\boldsymbol{r})=(1+\eta)\frac{N_{th}(\boldsymbol{r})}{T_1}, \quad (25)$$

where N_{th}/T_1 is the threshold pump rate; $N_{th}(\boldsymbol{r})$ is the spatial distribution of the inverse population density for the threshold pump rate; and η is the excess of the pump power over the lasing threshold. We assume that this excess is rather small ($\eta\ll 1$) and for simplicity consider the case, when the distribution $N_{th}(\boldsymbol{r})$ is virtually homogeneous [$N_{th}(\boldsymbol{r})\approx N_{th}=\text{const}$]. Because for $\eta\ll 1$ the intracavity field is small, Eqn (24) can be approximately written in the form

$$\frac{\partial N}{\partial t}=(1+\eta)\frac{N_{th}}{T_1}-\frac{N}{T_1}-\frac{aN_{th}}{T_1}\left[\sum_{1,2}|E_{1,2}|^2|u_{1,2}(\boldsymbol{r})|^2\right.$$

$$\left.+\sum_{1,2}E_{1,2}E^*_{2,1}(\boldsymbol{e}_{1,2}\boldsymbol{e}_{2,1})u_{1,2}(\boldsymbol{r})u^*_{2,1}(\boldsymbol{r})\exp(\pm 2ikz)\right]. \quad (26)$$

It is easy to derive from (26) the ordinary differential equations

$$T_1\frac{dN_1}{dt}=(1+\eta)N_{th}-N_1-aN_{th}\left(|E_1|^2C_1+|E_2|^2C_{12}\right),$$

$$T_1\frac{dN_2}{dt}=(1+\eta)N_{th}-N_2-aN_{th}\left(|E_1|^2C_{12}+|E_2|^2C_2\right), \quad (27)$$

$$T_1\frac{dN_{12}}{dt}=-N_{12}-2aN_{th}\beta C_{12}E_1E^*_2, \quad N_{21}=N^*_{12}$$

for the variables $N_{1,2}$ and N_{12}.
We introduced here the parameters

$$C_{1,2}=\int|u_{1,2}(\boldsymbol{r})|^4d\boldsymbol{r}, \quad (28)$$

$$C_{12} = \int |u_1(\boldsymbol{r})|^2 |u_2(\boldsymbol{r})|^2 \mathrm{d}\boldsymbol{r} \tag{29}$$

and the polarisation parameter

$$\beta = \int \frac{|\boldsymbol{e}_1 \boldsymbol{e}_2|^2 |u_1(\boldsymbol{r})|^2 |u_2(\boldsymbol{r})|^2 \mathrm{d}\boldsymbol{r}}{\int |u_1(\boldsymbol{r})|^2 |u_2(\boldsymbol{r})|^2 \mathrm{d}\boldsymbol{r}}. \tag{30}$$

We assume for simplicity in (16) that the shifts of eigenfrequencies due to rotation (22) are symmetric, i.e. $\Omega_1 = -\Omega_2 = \Omega$. Taking this into account, Eqn (16) can be rewritten in the form

$$\frac{\mathrm{d}E_{1,2}}{\mathrm{d}t} = -\frac{\omega}{2Q_{1,2}} E_{1,2} - \mathrm{i}\left(\omega_{\varepsilon 1,\varepsilon 2} \mp \frac{1}{2}\Omega\right) E_{1,2} + \frac{\mathrm{i}}{2} \tilde{m}_{1,2} E_{2,1}$$

$$+ \frac{\sigma L}{2T}(1 - \mathrm{i}\delta)(N_{1,2} E_{1,2} + N_{12,21} E_{2,1}). \tag{31}$$

By assuming that $C_{1,2} = C_{12} = 1$, $\omega_{\varepsilon 1,\varepsilon 2} = 0$ and $\boldsymbol{e}_{1,2}$ are independent of z, the system of equations (27), (31) with the accuracy to notation is equivalent to the equations of the standard vector SRL model written for a small excess of the pump over the threshold.

The calculation of coefficients $C_{1,2}$, C_{12} and β in the general case is a rather difficult problem. Paper [8] presents the method for calculating the parameters of a Gaussian beam with a complex astigmatism of the fundamental mode of an empty nonplanar ring resonator. The functions $u_{1,2}(\boldsymbol{r})$ calculated by this method prove to be equal to each other. The inequality of transverse distributions of counterpropagating waves in the ring cavity can be caused by the inhomogeneities of the active medium and errors in the resonator fabrication, which also should be taken into account in rigorous calculations. The polarisations of the ideal resonator can be calculated, as mentioned above, by using the Jones matrix method [9].

The system of equations obtained in this paper differs from the vector model equations considered in [4] in the case of spatially inhomogeneous distributions of the inverse population and the intracavity field. For the equivalent spatial field distributions of counterpropagating waves ($|u_1(\boldsymbol{r})| = |u_2(\boldsymbol{r})|$), due to the inversion and field inhomogeneity the optical nonreciprocity does not appear (frequency shifts $\omega_{\varepsilon 1,\varepsilon 2}$ prove to be equal for counterpropagating waves). In the case of nonequivalent spatial field distributions of counterpropagating waves, these frequency shifts are not equal, i.e. the cavity eigenfrequencies split. This does not contradict the optical nonreciprocity principle because this principle assumes the identity of counterpropagating waves.

3. Comparison of experimental results with the results of numerical simulation

We studied experimentally the characteristics of self-modulation oscillations of counterpropagating waves in the SRL and compared the obtained results with theoretical predictions based on the vector model described above. The experimental setup was completely similar to that used in [6]. The solid-state laser operated in the self-modulation regime of the first kind. In this regime, we measured the dependences of the phase difference of self-modulation intensity oscillations for counterpropagating waves (Fig. 1) and of intensity modulation depths (Fig. 2) on the pump excess over the threshold.

Some experimental effects cannot be explained within the framework of the standard model. One of these effects is the dependence of the phase shift of self-modulation oscillations on the pump excess over the threshold. To explain this effect in the standard model, it is necessary to assume that the difference of the cavity Q factors for counterpropagating waves depends on the value of this excess, which cannot be substantiated physically.

In the model presented in this paper, the inequality of coefficients $C_{1,2}$ appearing due to the difference between the transverse field distributions of counterpropagating waves leads to the inequality of gains for counterpropagating waves. Indeed, these coefficients enter Eqns (27) describing the saturation of the inverse population of the medium. The difference in the degrees of the inversion saturation leads to the inequality of gains for counterpropagating waves. This gives rise to an additional mechanism responsible for the change in the phase difference of self-modulation oscillations in counterpropagating waves (in the standard model, this phase difference appears only when the resonator Q factors are not equal). In addition, one can see from Eqn (16) that in the model under study in the absence of rotation or magnetic field (for $\Omega = 0$), the difference in the eigenfrequencies of the ring cavity appears for counterpropagating waves $\Delta\omega = \omega_{\varepsilon 1} - \omega_{\varepsilon 2}$ due to the inhomogeneities of the permittivity of the intracavity medium.

The numerical simulation based on our model gave good qualitative and quantitative agreement of experimental and theoretical results, which was impossible within the framework of the standard vector model. Some parameters in the numerical simulation were assumed equal to the laser parameters measured experimentally in [6]. The cavity bandwidth ω_c/Q determined from the relaxation frequency $\omega_r = (\eta\omega_c/QT_1)^{1/2}$ was 4.4×10^8 s^{-1}. In [6], the modulus $m/2\pi = (m_1 m_2)^{1/2}/2\pi \approx 332.6$ kHz and the phase difference $\theta = \theta_1 - \theta_2 = 0.648\pi$ for coupling coefficients were found from experimental parameters of self-modulation oscillations. These values were used in the numerical simulation in this paper. The parameters m_1, m_2, C_1, C_2, C_{12}, and β were varied in the numerical simulation. The best agreement between the numerical simulation and the experiment was obtained for $m_1/2\pi = 318$ kHz, $m_2/2\pi = 348$ kHz, $\beta = 0.405$, $C_1 = 0.998$, $C_2 = 0.99715$, $C_{12} = 0.997$. To describe the observed experimental dependences, it was necessary to introduce the splitting of ring-cavity eigenfrequencies $(\omega_{\varepsilon 1} - \omega_{\varepsilon 2})/2\pi = 20$ kHz. This splitting in the model under study can appear due to the inhomogeneities of the medium permittivity and the difference in the spatial field distributions of counterpropagating waves.

The experimentally measured intensity oscillograms of counterpropagating waves $I_{1,2}$ were processed by approximating them by the dependences $I_{1,2} = A_{01,02} + A_{1,2} \times \sin(\omega t + \varphi_{1,2})$, which allowed us to separate the useful signal from noise. The modulation depths $h_{1,2}$ were determined as the ratio $A_{1,2}/A_{01,02}$. Note also that the described experimental dependences of the phase shift of self-modulation oscillations and modulation depth of intensities of counterpropagating waves on the pump excess over the threshold were measured simultaneously.

Figure 1 shows the dependences of the phase shift $\Delta\varphi = \varphi_1 - \varphi_2$ of self-modulation oscillations of counter-

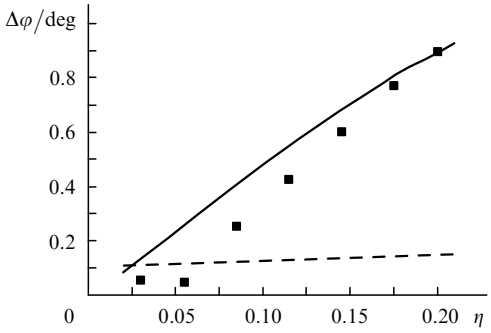

Figure 1. Experimental (squares) and calculated (curves) dependences of the phase shift of self-modulation oscillations of counterpropagating waves on the pump excess over the threshold. The solid curve is the result of simulations based on the described model, the dashed line is the prediction of the standard vector model ($C_{1,2} = C_{12} = 1$) [4].

propagating waves on the pump excess over the threshold. In simulations based on the standard model, it was assumed that the effective difference of Q factors of counterpropagating waves is

$$\frac{\Delta}{2\pi} = \frac{1}{4\pi}\left(\frac{\omega}{Q_2} - \frac{\omega}{Q_1}\right) = 1 \text{ kHz}.$$

One can see from Fig. 1 that in the case of the standard model the phase shift of self-modulation oscillations is independent of the pump excess over the threshold, which contradicts the experimental results, while the results of simulations based on the improved model described above well agree with the experimental data.

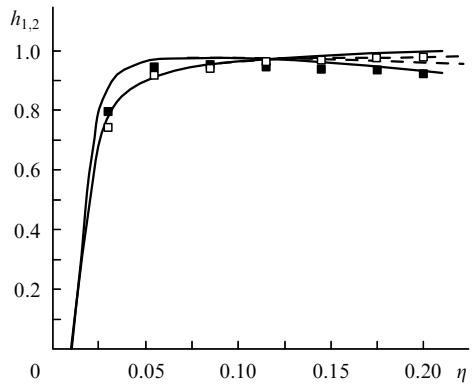

Figure 2. Experimental (squares) and calculated (curves) dependences of the modulation depths $h_{1,2}$ of counterpropagating waves on the pump excess over the threshold in the self-modulation regime of the first kind. The solid curve is the results of simulations based on the described model, the dashed line is based on the vector model [4].

Figure 2 shows the experimental and calculated dependences of the modulation depth of counterpropagating waves on the pump excess over the threshold in the self-modulation regime of the first kind. One can see that the model under study better describes the experimentally observed increase in the difference in modulation depths of counterpropagating waves with increasing the pump excess over the threshold.

4. Conclusions

We have obtained a system of ordinary differential equations in the vector model of solid-state ring lasers, which takes into account the inhomogeneities of the transverse distribution of the pump intensity and the intracavity field. Our study has shown that the difference in the transverse field distributions of counterpropagating waves in solid-state ring lasers can lead to the splitting of the cavity eigenfrequencies and to the appearance of an additional phase shift of self-modulation oscillations of counterpropagating waves. The model under study well describes the experimental dependence of the phase shift of self-modulation oscillations on the pump excess over the threshold.

Acknowledgements. This work was supported by the Russian Foundation for Basic Research (Grant Nos 07-02-00204 and 08-02-00217).

References

1. Kravtsov N.V., Lariontsev E.G. *Kvantovaya Elektron.*, **36**, 192 (2006) [*Quantum Electron.*, **36**, 192 (2006)].
2. Kravtsov N.V., Lariontsev E.G. *Kvantovaya Elektron.*, **34**, 487 (2004) [*Quantum Electron.*, **34**, 487 (2004)].
3. Mamaev Yu.A., Milovskii N.D., Turkin A.A., Khandokhin P.A., Shirokov E.Yu. *Kvantovaya Elektron.*, **27**, 228 (1999) [*Quantum Electron.*, **29**, 505 (1999)].
4. Boiko D.L., Kravtsov N.V. *Kvantovaya Elektron.*, **25**, 880 (1998) [*Quantum Electron.*, **28**, 856 (1998)].
5. Boiko D.L., Kravtsov N.V. *Kvantovaya Elektron.*, **27**, 27 (1999) [*Quantum Electron.*, **29**, 309 (1999)].
6. Zolotoverkh I.I., Kravtsov N.V., Lariontsev E.G., Firsov V.V., Chekina S.N. *Kvantovaya Elektron.*, **37**, 1011 (2007) [*Quantum Electron.*, **37**, 1011 (2007)].
7. Arnand J.A., Kogelnik H. *Appl. Opt.*, **8**, 1687 (1969).
8. Golovin I.V., Kovrigin A.I., Konovalov A.N., Laptev G.D. *Kvantovaya Elektron.*, **22**, 461 (1995) [*Quantum Electron.*, **25**, 436 (1995)].
9. Nilson A.C., Gustafson E.K., Byer R.L. *IEEE J. Quantum Electron.*, **25**, 767 (1989).